Journal of Marine Research, 60, 477–498, 2002

On the relative importance of the remote and local wind effects on the subtidal exchange at the entrance to the Chesapeake Bay

by Kuo-Chuin Wong[1] and Arnoldo Valle-Levinson[2]

ABSTRACT

Water velocity data from acoustic Doppler current profilers and electromagnetic current meters deployed at six separate locations across the entrance of the Chesapeake Bay from mid-April to early July of 1999 and from early September to mid-November of 1999 were used in conjunction with wind velocity and sea level records to describe the characteristics of the wind-induced subtidal volume exchange between the bay and the adjacent continental shelf. The current measurements were used to estimate volume fluxes associated with the local and remote wind-induced bay-shelf exchange over time scales of 2–3 days. The results show that at these relatively short subtidal time scales (1) the net flux integrated over the entrance to the estuary adequately describes the unidirectional (either inflow or outflow over the entire cross-section) barotropic volume flux associated with the coastally forced remote wind effect, (2) during the first deployment there is always a bi-directional exchange pattern (inflow and outflow existing simultaneously over different parts of the cross-section) superimposed on the sectionally integrated unidirectional exchange, (3) the magnitude of the bi-directional transport associated with the local wind effect may be a significant fraction of the unidirectional transport associated with the remote wind effect, and (4) the relative importance of the local wind effect in producing estuary-shelf exchange changes appreciably with season, depending on the characteristic frequency of the wind events and the degree of stratification in the estuary.

1. Introduction

Wind events have long been recognized for their considerable influence on the subtidal variability in estuaries (e.g. Pollak, 1960). Weisberg and Sturges (1976) and Weisberg (1976) found that wind played a dominant role in forcing the subtidal currents in the Providence River and the west passage of Narragansett Bay. In a series of studies in Chesapeake Bay and some of its tributaries, Wang and Elliott (1978), Elliott (1978), and Wang (1979a, b) showed that the subtidal sea level fluctuations in the Chesapeake were forced primarily by the up-bay propagation of alongshore wind-induced coastal sea level

1. College of Marine Studies, University of Delaware, Newark, Delaware, 19716, U.S.A. ***e-mail: kuo@newark.cms.udel.edu***

2. Center for Coastal Physical Oceanography, Department of Ocean, Earth and Atmospheric Sciences, Old Dominion University, Norfolk, Virginia, 23529, U.S.A.

fluctuations. They also found that the response of the coupled Chesapeake Bay-continental shelf system to atmospheric forcing could largely account for the subtidal barotropic volume exchange in the lower bay. The importance of wind on subtidal current or sea level variability has also been demonstrated by Smith (1977, 1978) in Corpus Christi Bay, Texas and Kjerfve *et al.* (1978) in North Inlet, South Carolina.

In more recent years the wind-induced subtidal variability has been examined extensively in many different types of estuaries. These studies cover well-mixed estuaries such as Delaware Bay (Wong and Garvine, 1984; Wong, 1994), partially mixed estuaries such as Chesapeake Bay (Vieira, 1985, 1986; Goodrich *et al.,* 1987; Goodrich, 1988; Chuang and Boicourt, 1989; Valle-Levinson, 1995; Paraso and Valle-Levinson, 1996; Valle-Levinson and Lwiza, 1998) and San Francisco Bay (Walters, 1982; Walters and Gartner, 1985), and highly stratified estuaries such as Mobile Bay (Schroeder and Wiseman, 1986; Wiseman *et al.,* 1988; Noble *et al.,* 1996) and the Childs and Quashnet in Massachusetts' Waquoit Bay (Geyer, 1997). A large number of studies have also been conducted to address the wind-induced subtidal exchange process in coastal lagoons with restricted communication with the ocean (e.g. Wong and Wilson, 1984; Kjerfve and Knoppers, 1991).

Wind can induce subtidal variability in estuaries through a combination of remote and local effects. For the remote effect, winds on the continental shelf adjacent to an estuary can produce sea level fluctuations at the mouth of that estuary. Additional coastal sea level fluctuations at the mouth of the estuary, in the form of free waves propagating into the region of interest, may be generated by winds over the continental shelf far away from the estuary (Gill and Schumann, 1974; Noble and Butman, 1979; Wang, 1979c; Ou *et al.,* 1981). Regardless of the exact mechanism operating over the continental shelf, the remote wind effect imposes coastal sea level set-up or set-down at the mouth of the estuary. This coastal set-up (or set-down) can then force subtidal variability in the interior of the estuary. On the other hand, the local wind effect acts directly over the surface area of the estuary to produce subtidal variability within that system. The remote and local wind effects can produce very different patterns of exchange between the estuary and the continental shelf. The remote wind effect tends to produce unidirectional flow throughout the cross-section of the entrance to the estuary, with a coastal set-up producing an inflow, and a coastal set-down producing an outflow (Wong, 1994; Janzen, 2000; Janzen and Wong, 2002). In contrast, bi-directional flow is produced by the local wind effect, with inflow over part of the estuary's cross-section and outflow over the rest of the cross-section. Officer (1976) has examined the effect of steady-state local wind forcing on an idealized estuary with a rectangular cross section. He found the existence of down-wind current in the upper layer of the estuary and up-wind current in the lower layer, with zero sectionally-integrated transport. In estuaries with lateral depth variations, a number of analytical and numerical modeling studies (e.g. Csanady, 1973; Hunter and Hearn, 1987; Hearn *et al.,* 1987; Signell *et al.,* 1990; Wong, 1994; Glorioso and Davies, 1995; Friedrichs and Hamrick, 1996) and a laboratory study (Fischer, 1976) showed that down-wind current exists throughout the water column over the shallow areas along the shores and up-wind return flow exists mainly over the deep channel. In these studies the down-wind flow along the shores cancelled the up-wind flow in the channel, resulting in zero (or weak) sectionally averaged transport.

Garvine (1985) has demonstrated, through a sectionally integrated analytical model, that the shortness of most estuaries relative to the subtidal wavelength favors the remote wind effect over the local wind effect in producing subtidal sea level and sectionally-averaged current fluctuations in estuaries. However, the sectionally-integrated model could not provide information on the magnitude of the spatially variable bi-directional exchange induced by the local wind effect. More recently, the modeling study of Janzen and Wong (2002) indicates that the bi-directional exchange associated with the local wind effect in an estuary is not necessarily weaker than the remote wind-induced uni-directional exchange. This is consistent with the observational evidence that the local wind effect is quite significant in forcing bi-directional subtidal currents in Delaware Bay (Wong and Moses-Hall, 1998).

The ultimate goal of this study is to advance our knowledge of the wind-induced estuary-shelf subtidal exchange. The specific objective of this work is to document the relative importance of the remote and local wind effects in forcing the volume exchange between a major estuary (Chesapeake Bay) and the adjacent continental shelf over relatively short subtidal time scales of 2–3 days. This objective is accomplished by analyzing volume fluxes estimated from time series measurements of water velocity profiles, wind velocity and sea level at the entrance to the Chesapeake Bay.

2. Study area

Chesapeake Bay is a partially mixed coastal plain estuary. The physical processes in the lower bay over the subtidal time scales are influenced by a combination of atmospheric forcing, tidal rectification, buoyancy forcing, and bathymetry. Of these mechanisms, wind produces energetic variability at time scales of 2–5 days, while the tidally rectified current and the buoyancy-induced gravitational circulation generally operate over longer time scales. The bathymetry at the entrance to the bay is marked by two channels located near the southern and northern ends of the bay mouth transect (Fig. 1). The Chesapeake Channel to the south has a maximum depth of 30 m, and the North Channel has a depth of 14 m. The channels are separated by the Middle Ground, a relatively flat region of about 10 m depth located immediately to the north of the Chesapeake Channel, and by the Six-Meters Shoal located immediately to the south of the North Channel.

The prevailing winds in the lower Chesapeake Bay carry significant seasonal variability (Paraso and Valle-Levinson, 1996). Winds are typically from the northeast between late summer and early spring, while southwesterly winds dominate during the summer. The most energetic wind events are generally from the northeast or northwest during late autumn and winter, but strong southwesterly winds can occasionally be observed. There are modest spatial variations in the distribution of the wind field near the mouth of the bay.

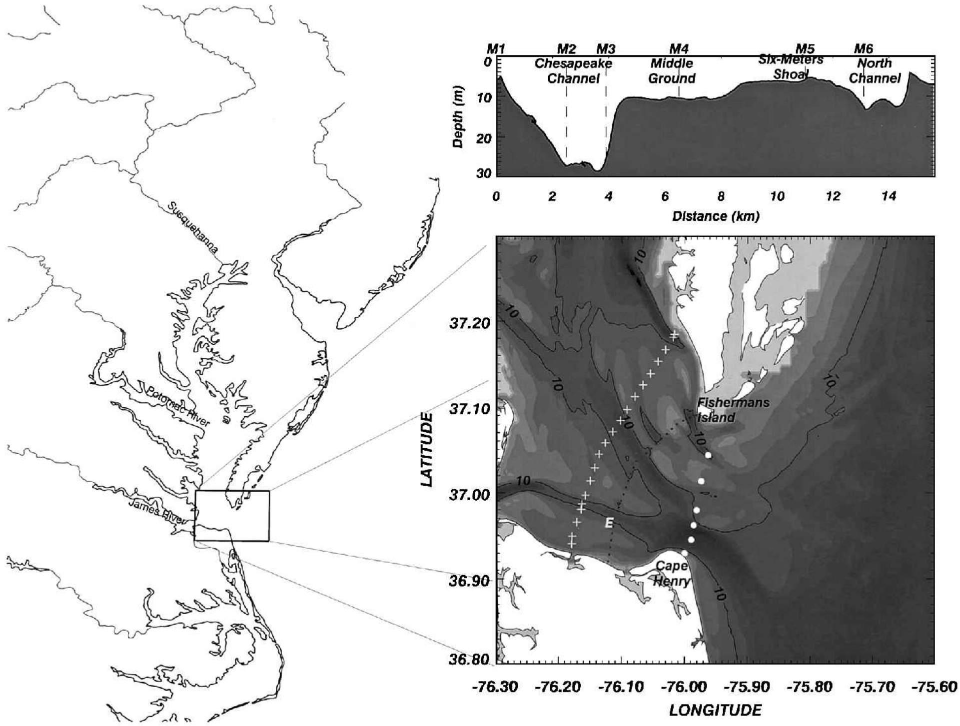

Figure 1. Map of the study area showing the lower Chesapeake Bay in the context of the eastern United States. The bathymetry of the lower Chesapeake Bay is shown with filled contours for which the darker tones denote deeper areas and with the 10 m isobath drawn for reference. The mooring locations are indicated by the small white circles at the entrance to the bay. The bathymetry of the sampling transect is shown in the upper insert with the appropriate labels for the bathymetric features discussed in the text and the corresponding position of the moorings M1, M2, M3, M4, M5, and M6. The white crosses indicate the monthly hydrographic transect conducted by the Center for Coastal Physical Oceanography (CCPO) at the Old Dominion University (ODU). The dark dashed line indicates the Chesapeake Bay Bridge Tunnel (CBBT). The symbol E denotes the location of the wind station at CBBT.

Paraso and Valle-Levinson (1996) have examined the winds at Chesapeake Bay Bridge Tunnel (CBBT, see Fig. 1) and at Chesapeake Light, located outside of the bay mouth. They concluded that the winds from these two locations, separated by a distance of about 25 km, show in-phase fluctuations with consistent orientations over 90% of the time. The magnitude of the wind at the offshore station at Chesapeake Light is about 2 m/s higher than that at CBBT 75% of the time. More recently, Reyes-Hernandez (2001) has examined the wind distributions at several locations in the lower bay near the bay mouth. These include CBBT and Chesapeake Light, as well as Kiptopeke, located to the northeast of CBBT, and Sewells Point, located to the southwest of CBBT. His study indicates that the winds at these stations show coherent fluctuations. The winds at CBBT are consistently stronger than those at Sewells Point and Kiptopeke (by 1 to 2 m/s), but are slightly weaker than the winds at Chesapeake Light.

Tidal forcing in the lower Chesapeake Bay is predominantly semidiurnal, with M_2 being the strongest constituent (Browne and Fisher, 1988). The interaction between M_2 and the other semidiurnal tidal constituents (N_2 and S_2) generates fortnightly and monthly variability in the tidal currents. This type of long-term, tidally induced variability has also been observed in other estuaries such as Delaware Bay (Münchow *et al.,* 1992).

Buoyancy forcing to the lower Chesapeake Bay is dominated by discharges from the Susquehanna, Potomac, and James rivers. The highest discharge is typically observed in March and April, and the lowest discharge occurs in August and September. As a result, the mean surface salinity is lowest throughout the bay in April–May and highest in September–November, roughly one month after the river discharge extremes. The mean discharge into the bay is about 2500 m^3/s (Goodrich, 1988).

Characterization of the bay-shelf exchange at different times of the year has been done at high spatial resolution in the study area using short-term (1 day) acoustic Doppler current profiler (ADCP) tows (Valle-Levinson *et al.,* 1998). That study examined two main scenarios of water exchange under southwesterly and non-southwesterly wind conditions. However, those two scenarios were drawn from short time series and under relatively weak (<10 m/s) wind forcing conditions. Therefore, the previous study is inadequate to elucidate the characteristics of the local and remote effects on the water exchange under strong and variable wind forcing conditions. The long-term (two separate ~75-day surveys) measurements presented here allow a more detailed examination of the wind-induced bay-shelf subtidal exchange and an assessment of the relative importance of the remote and local wind effects in producing the observed exchange.

3. Data collection

Two ~75-day deployments of moored instrumentation were carried out in the spring-summer and in the autumn of 1999. The typical seasonal variation in river discharge favors stronger buoyancy forcing in spring than in autumn, and the 1999 conditions were consistent with that trend. Instrumentation deployed consisted of five upward-looking bottom-mounted acoustic Doppler current profilers (ADCPs) with pressure sensors and three point current-meters. This instrumentation was distributed in six moorings across the entrance to the Chesapeake Bay as shown in Table 1.

For the spring deployment the National Oceanic and Atmospheric Administration (NOAA)'s ship Ferrel was used to deploy five bottom-mounted RD Instruments "work-horse" ADCPs at M1, M2, M3, M4, and M6 (see Fig. 1) during April 19–22, 1999. Two Inter Ocean S4 current meters, one at mid-depth (~2.5 m from the surface) and one at ~1 m above the bottom, were used for mooring 5. Another near-bottom S4 current meter was deployed at mooring 4. A Benthos acoustic pop-up buoy was deployed at each site to provide a marker for the mooring location during the recovery effort. After a 75-day deployment, the recovery of the moored instruments was initiated on July 6. With a team of

Table 1. Details on each instrument deployment. Times are given in GMT. The Dep1 column indicates the total water column depth. The Dep2 column indicates the depth at which the instrument was deployed. All instruments recorded at 15-minute-ensembles. ADCPs recorded 200 pings per ensemble.

	Mooring	Instrument	Latitude (N)	Longitude (W)	Day & Time in	Dep1 (m)	Dep2 (m)
April-July	1	ADCP/WH-1200	36° 55.7891′	75° 59.9946′	20/04/99 1645	7.3	7
(Spring)	2	ADCP/WH-600	36° 56.7269′	75° 59.3762′	20/04/99 1736	23.5	23
1999	3	ADCP/WH-300	36° 57.7378′	75° 59.1358′	19/04/99 2129	22.9	22.5
	4	ADCP/WH-600	36° 58.7881′	75° 58.8509′	22/04/99 1315	10.4	10
	5	S4	37° 00.8090′	75° 58.4200′	19/04/99 1605	6.7	3
	5	S4	37° 00.8090′	75° 58.4200′	21/04/99 1500	6.7	5
	6	ADCP/WH-600	37° 02.6349′	75° 57.7698′	19/04/99 1802	12.8	12.5
Sep-Nov	1	ADCP-WH-1200	36° 55.7061′	75° 59.8110′	9/09/99 1630	6.1	5.8
(Autumn)	2	ADCP/WH-600	36° 56.7707′	75° 59.2949′	9/09/99 1730	24.4	24.1
1999	3	ADCP/WH-300	36° 57.7708′	75° 59.1406′	9/09/99 1518	22.3	22
	4	ADCP/WH-600	36° 58.9817′	75° 58.8900′	9/08/99 1547	10.7	10.4
	5	S4	37° 00.4531′	75° 58.1754′	9/08/99 1458	6.4	3
	5	S4	37° 00.4531′	75° 58.1754′	9/09/99 1520	6.4	5
	6	ADCP/WH-600	37° 02.5809′	75° 57.7663′	9/08/99 1356	12.2	11.9

divers, it took more than a week to recover all the moored instruments since only one of the pop-up buoys was able to send a marker to the surface upon command. In the fall, the survey was repeated with the deployment of five bottom mounted RDI workhorse ADCPs and three S4s from the Sea Search during September 7–9, 1999. After a ~70-day deployment, the recovery of the moored instruments, which lasted for about a week, was initiated on November 9. Details about the mooring deployment/recovery can be found in Valle-Levinson *et al.* (2001).

Hourly wind velocity data were obtained from the Chesapeake Bay Bridge Tunnel (Fig. 1). Sea surface elevations were derived from detrended and demeaned pressure data recorded by the ADCP. All time series data were passed through a Lanczos filter with a half-power point of 25 hr to eliminate the high frequency tidal variability, as this study concentrates exclusively on the subtidal signals.

4. The tidally rectified current and gravitational circulation

The observed low-pass filtered subtidal currents include not only the wind-induced variability but also the tidally rectified current and gravitational circulation, so the effects of the latter two need to be removed in order to isolate the wind-induced effect. Tidal rectification can produce a mean current as well as low frequency currents at fortnightly and monthly time scales (Ianniello, 1977, 1979). MacCready (1999) has shown that for estuaries of intermediate depth (about 20 m) the system can take significant time (two weeks or longer) to adjust to changes in river flow. This type of long adjustment time scale has also been observed at the mouth of Delaware Bay (Garvine, 1991). On the other hand,

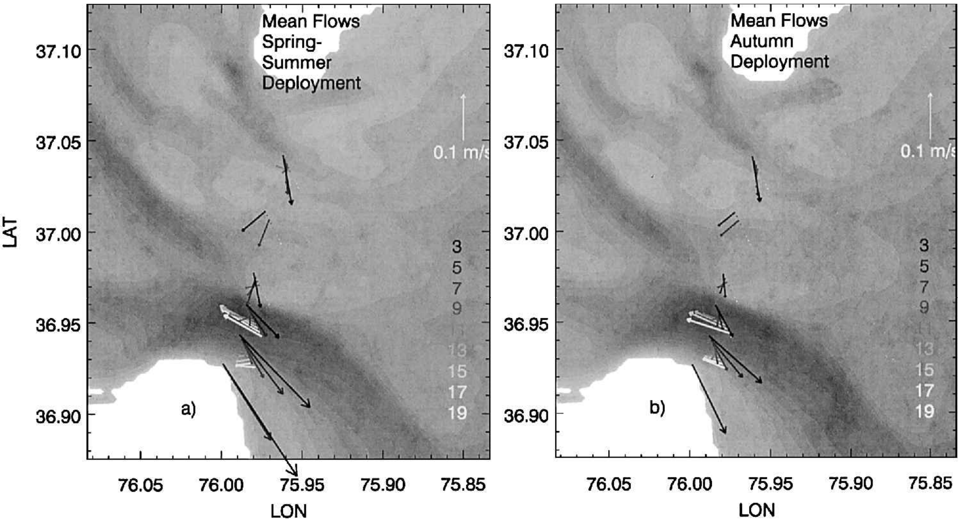

Figure 2. The spatial distribution of the mean currents from the spring-summer (a) and the autumn (b) deployments.

the effect of winds on subtidal currents is important over shorter subtidal time scales of 2–5 days (Wong, 2002). Since tidally rectified current and gravitational circulation typically operate over long time scale, it is instructive to examine the spatial distribution of the mean current at the moorings. Figure 2 shows that the mean flow patterns are highly consistent between the two deployments. Both show surface outflow and bottom inflow over the main channel and significant transverse flow over the shallower, northern part of the bay mouth. The volume flux associated with the mean outflow is about 0.3×10^4 m^3/s, and that associated with the mean inflow, is about -0.2×10^4 m^3/s. This mean outflow estimate is of the same order of magnitude as the one made by Goodrich (1987) in an earlier study. The fact that the mean flows are somewhat stronger during the first survey may be attributed to the stronger buoyancy forcing in the spring relative to the situation in the fall. Figure 3 shows the salinity distribution across the mouth of the Chesapeake Bay during June and September, 1999. These data are derived from the monthly hydrographic cruises conducted by the Center for Coastal Physical Oceanography (CCPO) at the Old Dominion University (ODU). The hydrographic transect does not overlap the mooring line exactly, but the two lines are less than 10 km apart (Fig. 1), and the hydrographic survey should adequately represent the transverse salinity distribution near the entrance of the bay. It is evident from this figure that stronger buoyancy forcing in June has resulted in lower salinity values and higher lateral and vertical salinity gradients than the conditions in September. The highly consistent nature of the mean flow pattern supports the approach of removing the mean currents of each survey from the observed subtidal currents in order to isolate the wind-induced flow.

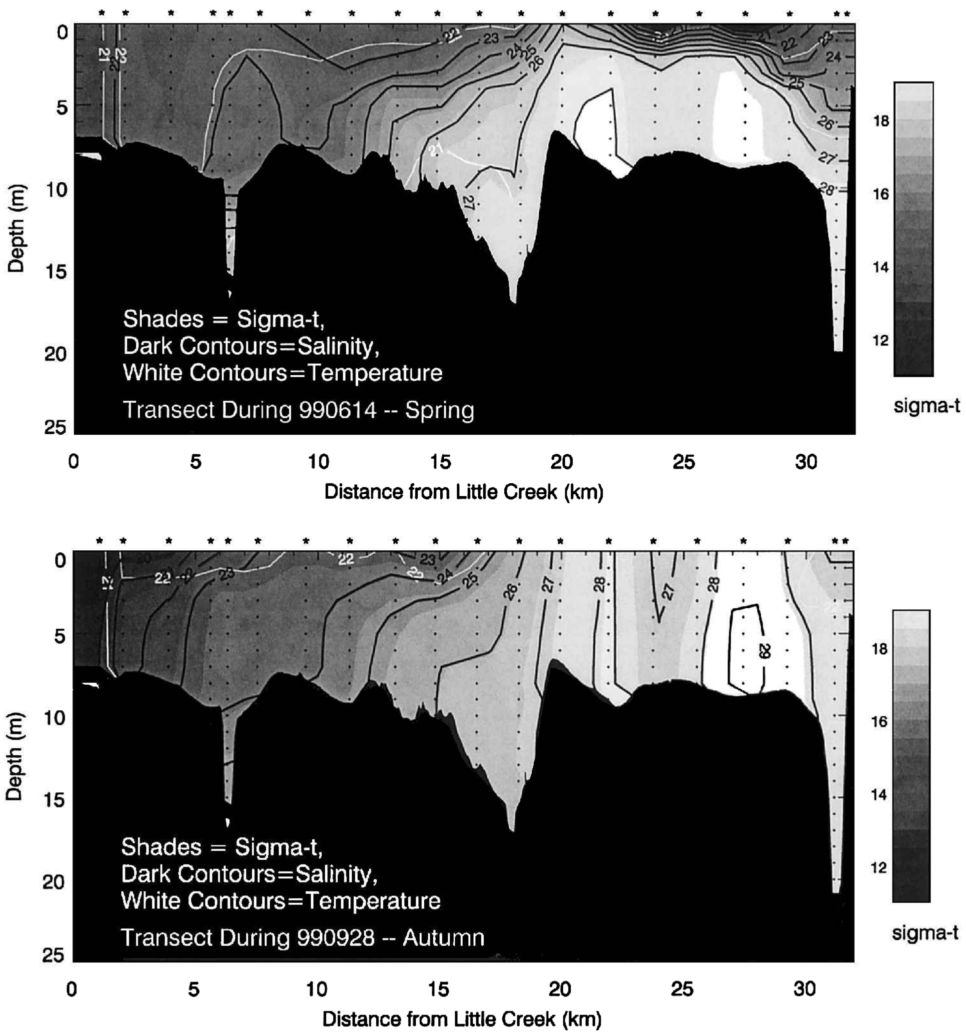

Figure 3. The salinity, temperature, and density (sigma-t) distributions along the CCPO monthly hydrographic transect at the mouth of Chesapeake Bay on June 14, 1999 (a) and September 28, 1999 (b). The view is up-bay, with the shore near Cape Henry (Little Creek) to the left.

5. Wind-induced volume flux

After subtracting the mean currents from the observed subtidal currents, the analysis is further simplified by focusing only on the current component that is perpendicular to the mooring transect across the bay mouth, with positive current indicating outflow and negative current indicating inflow. This simplification is justified because the main objective of the present study is to examine the volume exchange between the bay and the shelf. With the vertical profiles of the current at six different locations across the bay mouth

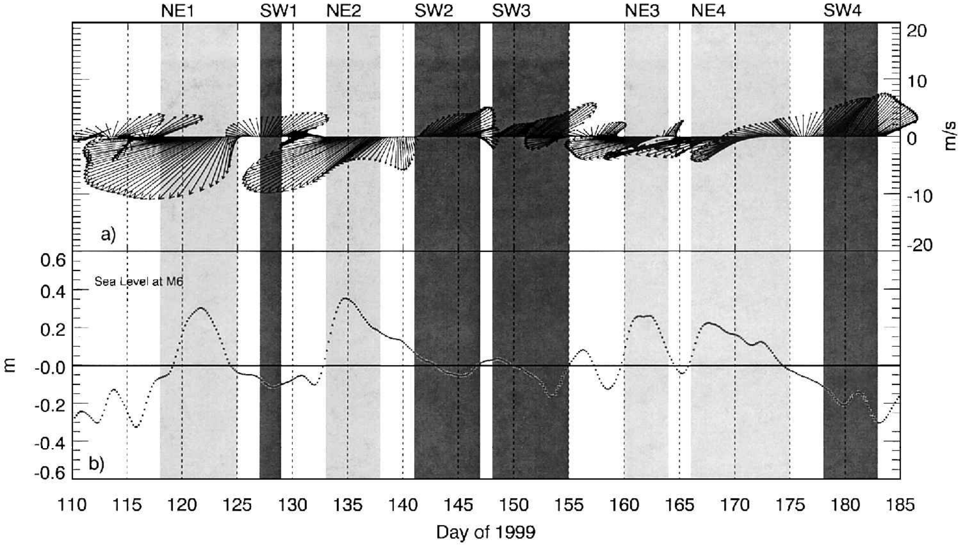

Figure 4. Time (GMT) series during the spring-summer deployment of wind velocity (a) (in meters per second) and low-passed sea level (b) (in meters) in the lower bay. Wind velocities in (a) point in the direction toward which they blew. The shaded bands represent the most energetic northeasterly (NE) or southwesterly (SW) wind pulses. Sea level at the mooring site was obtained from the ADCP pressure sensor.

transect, we can estimate both the sectionally integrated flux through the transect and the magnitude of the inflow and outflow associated with the wind-induced motion at different parts of the transect. To calculate volume flux, the currents from the mooring sites were interpolated throughout the transect based on Delaunay triangulations as described by the Interactive Data Language (IDL) software package. The interpolation produces current values at 500 m (horizontal) by 0.5 m (vertical) cells across the transect. Volume flux through each cell is computed by multiplying the velocity at that cell with the area of the cell, and the net volume flux through the entire transect (Q_{net}) is computed by summing the fluxes through all the cells. To examine the effect of bi-directional exchange typically associated with the local wind effect, fluxes associated with the inflow (Q_{in}) and outflow (Q_{out}) at different parts of the bay entrance cross-section are also summed separately. It follows that $Q_{in} + Q_{out} = Q_{net}$.

a. Spring-summer deployment

During the first (spring-summer) deployment, wind forcing was mostly northeasterly (NE) and southwesterly (SW) (Fig. 4a). Throughout the 75-day observation period there were 8 low frequency wind pulses that exceeded 5 m/s at CBBT: 4 NE wind pulses and 4 SW wind pulses. Northeasterly winds caused sea level to rise in the lower bay and southwesterly winds caused sea level to fall (Fig. 4b), consistent with the effect of coastal

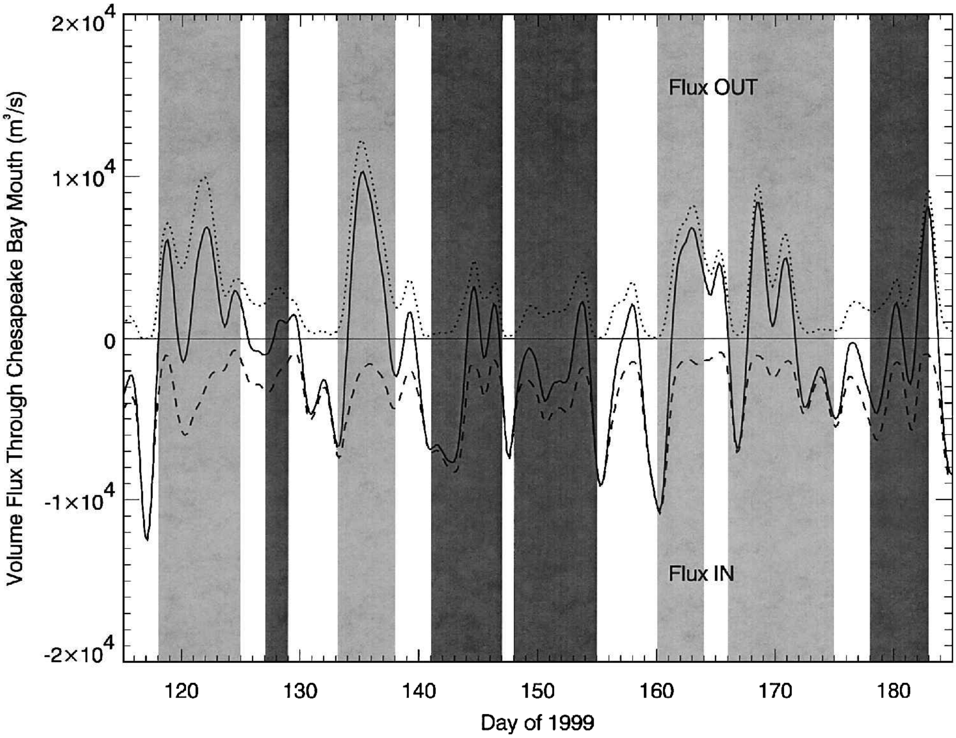

Figure 5. Time (GMT) series during the spring-summer deployment of subtidal volume flux out of the bay (Q_{out}), flux into the bay (Q_{in}), and the net flux through the bay entrance ($Q_{net} = Q_{in} + Q_{out}$). The dotted line indicates Q_{out}, the dashed line indicates Q_{in}, and the solid line indicates Q_{net}.

Ekman forcing where downwelling favorable NE wind produces coastal set-up and upwelling favorable SW wind produces coastal set-down. Both wind components (easterly and northerly) showed a strong correlation with sea level. A multiple regression that included both components of the wind explained 85% of the sea level variance at the entrance of the bay. The wind-induced subtidal current has a very complicated transverse structure across the bay entrance. Valle-Levinson *et al.* (2001) have documented the spatial variability of the currents associated with selected NE and SW wind events during this deployment. The focus of the present study, however, is the volume flux associated with the inflow, outflow, and net transport. Through the identification of the uni-directional and bi-directional transport pattern, the relative importance of the local and remote wind effects in forcing the volume exchange between the bay and the adjacent continental shelf over time scales of 2–3 days can be established.

Figure 5 shows the sectionally integrated net flux Q_{net} through the bay entrance, as well as Q_{in} and Q_{out}. All three fluxes show fluctuations of up to $\pm 1.0 \times 10^4$ m^3/s over typical time scales of 2–3 days. It is interesting to note that while either inflow or outflow may

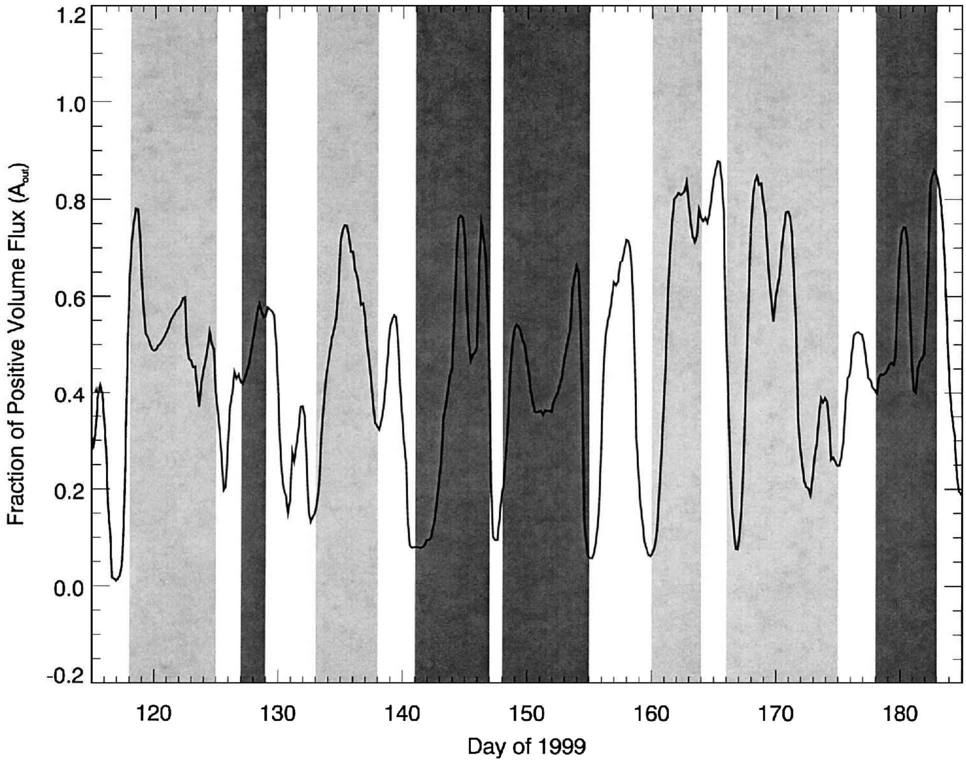

Figure 6. Time (GMT) series of the fractional area (A_{out}) of the bay entrance cross-section with water flowing out of the bay during the spring-summer deployment. $A_{out} = 1$ indicates outflow everywhere along the cross-section and $A_{out} = 0$ indicates inflow everywhere.

dominate during particular wind events, neither Q_{in} nor Q_{out} would completely vanish, indicating the existence of some degree of bi-directional estuary-shelf exchange, with inflow occurring over parts of the bay mouth transect and outflow occurring over the remaining cross-section. Another way of characterizing the bi-directionality of the transport is to compute the fraction of the cross-sectional area that is occupied by the outflow A_{out} (Fig. 6). The fraction of the cross-sectional area that carries inflow is thus $A_{in} = 1 - A_{out}$. It can be seen that A_{out} never reaches 1 or 0, indicating that even during events when the overall transport is dominated by either the inflow or the outflow, there is always an opposing flow operating over part of the cross-section. As a matter of fact, A_{out} varies primarily between 0.3 and 0.7, indicating the presence of a significant bi-directional flow field under most wind events during this survey.

In order to assess the characteristics of the wind-induced volume exchange between Chesapeake Bay and the adjacent continental shelf, it is necessary to relate the computed fluxes (Q_{in}, Q_{out}, and Q_{net}) to the fluxes associated with the remote (Q_R) and local $Q(_L)$ wind effects. The remote wind effect pumps the estuary by imposing coastal sea level fluctuations at the entrance of the estuary. To lowest order, the sea level in the interior of the estuary simply co-oscillates with the coastal sea level, thus producing a remotely forced barotropic volume exchange (Q_R) through the entrance of the estuary (e.g. Garvine, 1985; Janzen, 2000). Using scaling analysis, Garvine (1985) indicated that the remote wind effect should dominate the local wind effect in producing the sectionally-integrated transport in estuaries. Following that analysis, the sectionally integrated volume flux may be a good approximation for the volume flux induced by the remote wind effect, or $Q_{\text{in}} + Q_{\text{out}} = Q_{\text{net}} \cong Q_R$.

In addition to estimating the remotely forced volume flux Q_R based on a calculation of the sectionally integrated transport derived from current measurements, Q_R can also be estimated from coastal sea level based on the continuity requirement (Goodrich, 1987; 1988). Assuming that to lowest order the sea level in the interior of the estuary follows that at the open boundary with no phase lag or attenuation, the barotropic volume flux through the entrance of the bay can be estimated as $A\partial\eta/\partial t$, where A is the surface area of the bay (8.0×10^9 m^2), η is sea level at the mouth and t is time. A comparison between $A\partial\eta/\partial t$ and Q_{net} (Fig. 7) shows that there are significant differences between these two fluxes at times. This is not surprising, as the calculation of either quantity to approximate Q_R involves many assumptions. Despite these limitations, however, a common pattern emerges where these two separate fluxes show similar fluctuations with comparable magnitudes during many wind events. This suggests that the sectionally integrated barotropic transport is a reasonable proxy for the volume flux forced by the remote wind effect over the entire cross-section, or

$$Q_{\text{net}} \cong Q_R.$$

To assess the relative importance of the remote and local wind effects on volume exchange, it is postulated that

$$Q_{\text{in}} + Q_{\text{out}} = Q_{\text{net}} = Q_R \tag{1}$$

$$Q_{\text{out}} = Q_{L1} + Q_{R1} \tag{2}$$

$$Q_{\text{in}} = Q_{L2} + Q_{R2} \tag{3}$$

Eq. (1) simply states that the sectionally-integrated net volume flux is caused by the remote effect. Eq. (2) states that the volume flux over the part of the cross-section where the current is flowing out of the estuary is forced by a combination of the local (Q_{L1}) and the remote (Q_{R1}) wind effect. Eq. (3) states similar properties for the part of the cross-section which carries inflow. There are three equations with four unknown variables (Q_{L1}, Q_{R1}, Q_{L2}, and Q_{R2}), so an additional condition is required to separate the contributions of the remote and local wind effects. Since the sum of the remote wind effect over the inflow and outflow regions has to be equal to the total remote effect acting over the entire cross-section, it follows from Eq. (1) that $Q_{R1} + Q_{R2} = Q_R$. At any given instance in time Q_R represents a unidirectional flow throughout the entire cross-section, so Q_{R1} can be written

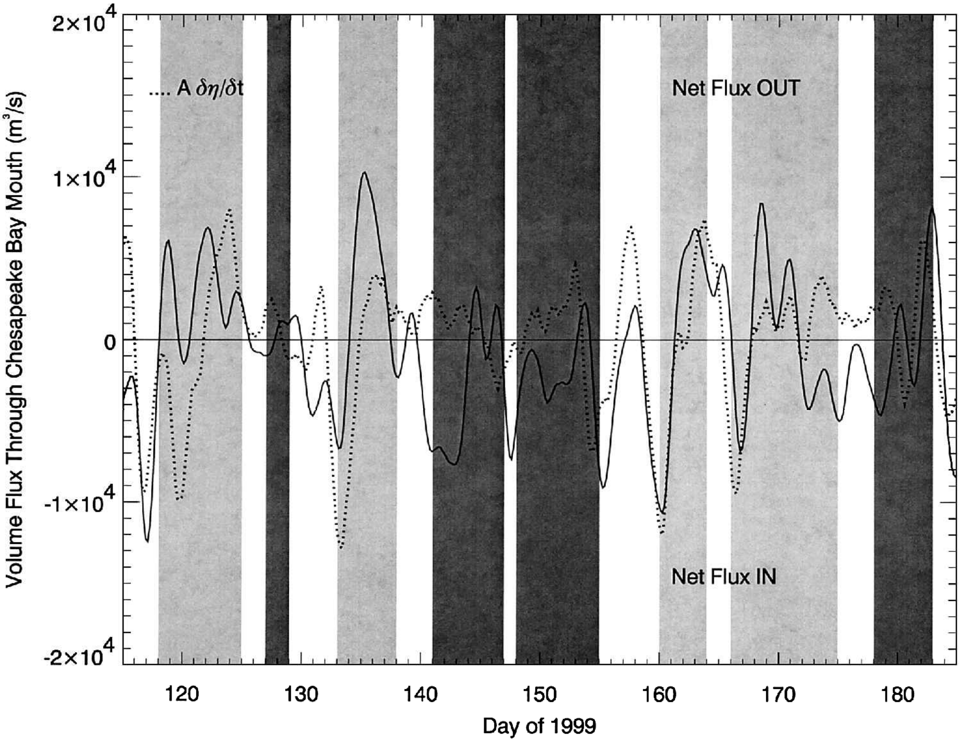

Figure 7. A comparison between the sectionally integrated net flux (Q_{net}), in solid line, and the barotropic flux estimated from the continuity requirement ($A\partial\eta/\partial t$), in dotted line, during the spring-summer deployment.

as αQ_R where α indicates the fraction of Q_R that is distributed over the outflow region of the cross-section. It follows that $0 \leq \alpha \leq 1$ and $Q_{R2} = (1 - \alpha)Q_R$. Eqs. (2) and (3) can now be written as

$$Q_{out} = Q_{L1} + \alpha(Q_{in} + Q_{out}) \tag{4}$$

$$Q_{in} = Q_{L2} + (1 - \alpha)(Q_{in} + Q_{out}). \tag{5}$$

As stated earlier, an additional independent condition is required to solve for the contribution of the local wind effect. Here one would need to know α, the fraction of the total remotely forced uni-directional volume flux that should be assigned to the part of the cross-section that carries outflow. As an approximation, A_{out}, the fractional area of the cross-section that carries outflow, is used to substitute for α. This approximation basically assumes that the effect of remotely forced volume exchange is distributed uniformly across the transect. With this approximation, it is straightforward to compute the effect of local wind as $Q_{L1} = Q_{out} - A_{out}(Q_{in} + Q_{out})$ and $Q_{L2} = Q_{in} - (1 - A_{out})(Q_{in} + Q_{out})$. Since

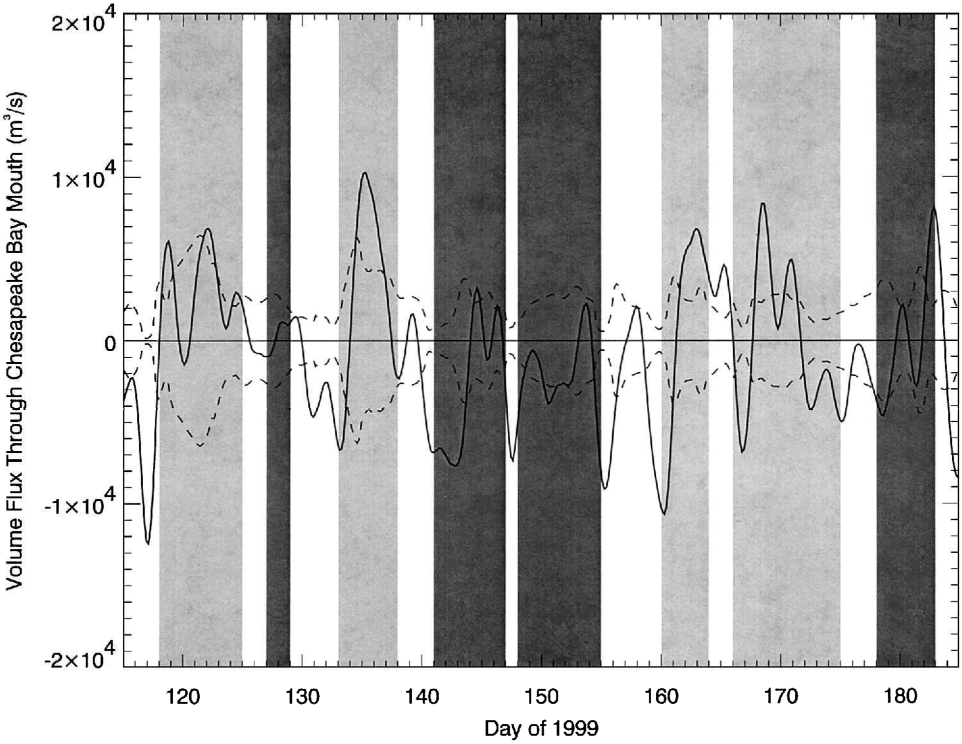

Figure 8. A comparison between the volume flux induced by the remote wind effect (solid line) and that induced by the local wind effect (dashed line) during the spring-summer deployment.

the local wind effect does not contribute to the sectionally integrated volume flux (Eq. 1), it follows that $Q_{L1} + Q_{L2} = 0$ (Fig. 8). For most wind events, the magnitude of the local wind-induced volume flux is about half of that induced by the remote wind effect. This indicates that Q_L (bi-directional volume flux induced by the local wind effect) will significantly reinforce Q_R (uni-directional volume flux induced by the remote wind effect) over part of the cross-section, and the two will counteract each other over the rest of the cross section. In certain wind events such as the one associated with the NE winds on day 122, the magnitude of Q_L is comparable to that of Q_R. Under other events such as the one with the SW winds centering on day 150, the magnitude of Q_L was even greater than Q_R.

b. Autumn deployment

During the second (autumn) deployment, winds were predominantly northwesterly (NW) and southwesterly (SW) (Fig. 9a). In this ~70-day period of observations four NW wind pulses caused consistent sea level and flow variations. Three SW wind pulses produced similar responses to those observed in the Spring-Summer deployment. The passage of Hurricane Floyd represents a major wind event. During that time period the

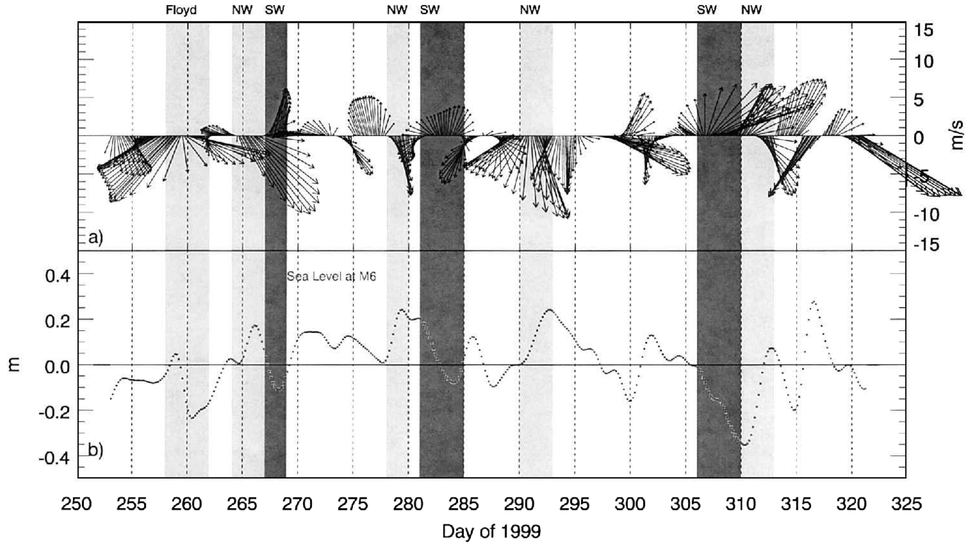

Figure 9. Same as Figure 4 except for the autumn deployment.

winds shifted rapidly from the northeast to the northwest, producing a sea level response comparable to that induced by NE winds.

During the entire autumn deployment wind pulses were more variable and of shorter duration than those in the first deployment. This resulted in rapid variations of subtidal sea level (Fig. 9b) that had a de-correlation time scale of $\sim$1 day, in contrast to the spring deployment that exhibited a de-correlation time scale of $\sim$2 days. The largest sea level set-up during the autumn deployment was related to NW winds, while the largest sea level set-down was again associated with SW winds. An exception to these patterns occurred around September 15–16 (days 258–259). With the passage of Hurricane Floyd over the area at that time, rapidly changing strong winds produced a rapid increase and subsequent decrease of sea level in less than 2 days (Valle-Levinson *et al.,* 2000).

Using the same method described before, the subtidal fluctuations in Q_{in}, Q_{out}, and Q_{net} are computed for the second deployment. The volume fluxes show fluctuations with magnitudes up to $\pm 2.0 \times 10^4$ m^3/s, except for the event associated with the passage of Hurricane Floyd (day 260) when the volume flux exceeded 4.0×10^4 m^3/s (Fig. 10). These values were more than a factor of 2 stronger than the ones observed in the first deployment. Furthermore, during the second deployment there are many instances where the exchange throughout the entire cross-section is completely dominated by either the outflow (e.g. day 260, Hurricane Floyd) or the inflow (e.g. day 312). In these instances the flow is essentially unidirectional throughout the bay entrance. This is also evident from the temporal variations of A_{out}, the fractional area of the bay entrance with water flowing out of the system (Fig. 11). On day 260 when outflow dominates the bay-shelf exchange $A_{\mathrm{out}} \approx 1$, and on day 312 when inflow dominates the exchange $A_{\mathrm{out}} \approx 0$. During much of the second

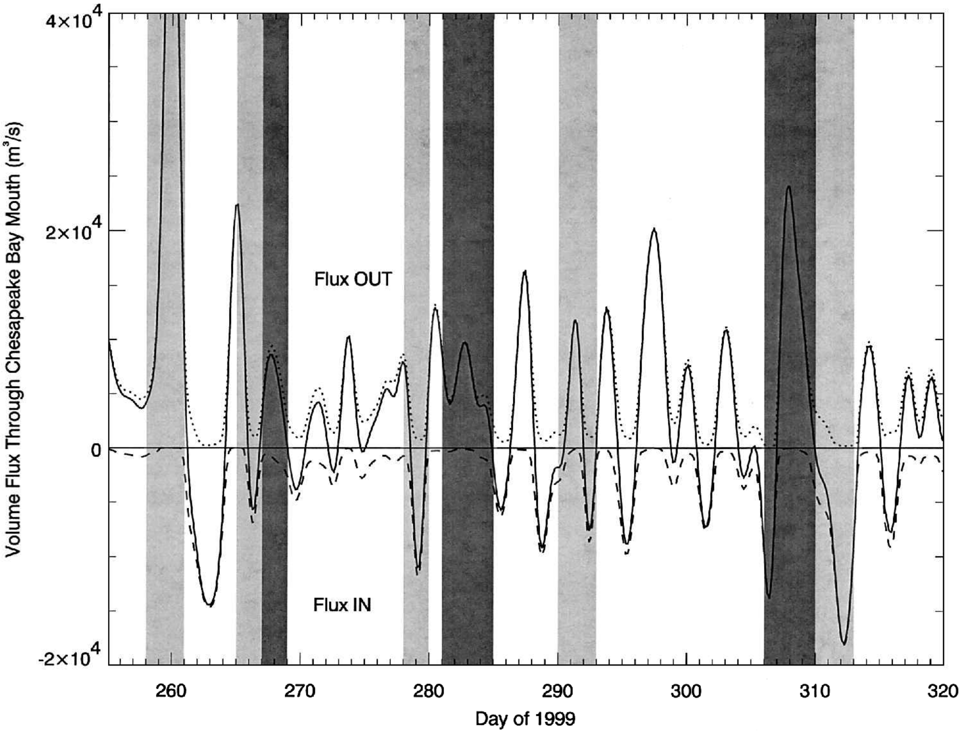

Figure 10. Same as Figure 5 except for the autumn deployment.

deployment A_{out} fluctuates between 0 and 1, indicating the existence of alternating patterns of near unidirectional inflow or outflow along the entire cross-section of the bay entrance. Given this type of exchange pattern, it is not surprising that Q_L (bi-directional volume flux from the local wind effect) was much weaker than Q_R (unidirectional volume flux from the remote wind effect). (Fig. 12).

6. Discussion

This study shows that the bi-directional transport induced by the local wind effect can contribute significantly to the subtidal exchange between a major coastal plain estuary and the adjacent continental shelf. This reinforces findings from earlier studies in systems such as the Delaware Bay (Wong and Moses-Hall, 1998; Janzen, 2000) about the importance of the local wind effect relative to the remote wind effect. Even though the local wind effect does not contribute to any net volume exchange, it may have a significant impact on the exchange of dissolved and suspended material between the estuary and the coastal ocean, as the distribution of the waterborne material in the outflow may be quite different from that in the inflow. In this respect the bi-directionality of the local wind-induced exchange can be compared to the buoyancy forced gravitational circulation which also does not

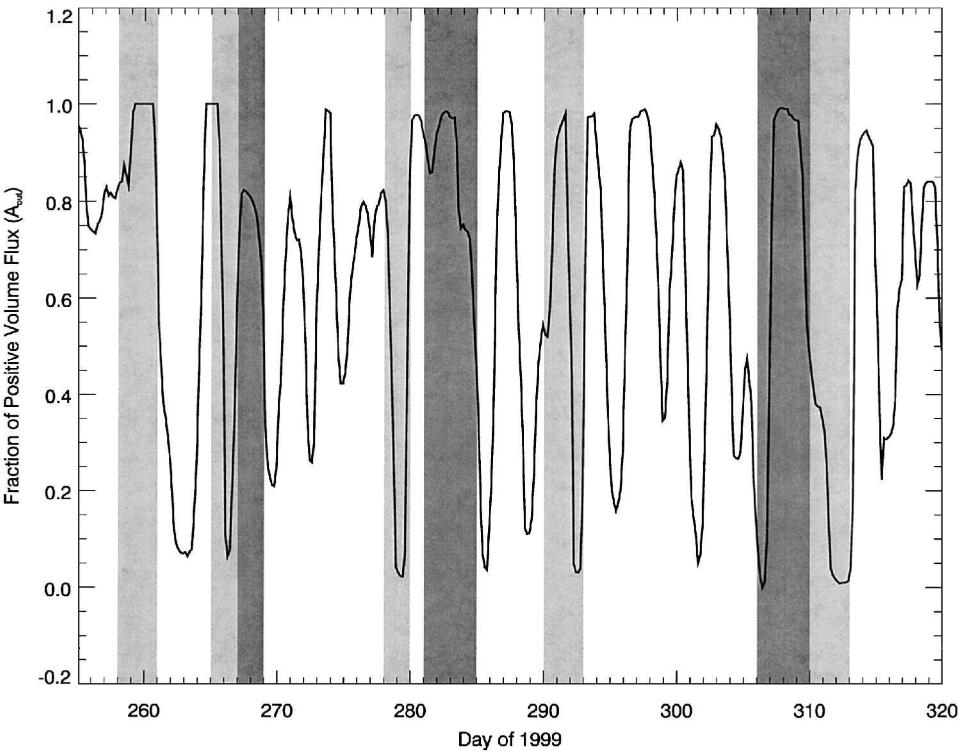

Figure 11. Same as Figures 6 except for the autumn deployment.

contribute much to the net volume exchange but can be quite important to the material exchange. Since the bi-directional exchange associated with the local wind cannot be readily derived from sea level measurements alone, current measurements with sufficient spatial resolution are crucial in determining the overall contributions of the remote and local wind effects to the exchange process between an estuary and the adjacent shelf.

The present study also shows that the relative importance of the remote and local effect exhibits significant seasonal variability. There are many possible reasons for the weaker local wind effect in the second (autumn) deployment compared with the first (spring) deployment. First of all, during the entire autumn deployment wind pulses were more variable than in the first deployment and also of shorter duration. This means that the characteristic frequency scale (ω) of the wind is higher in autumn than in spring. The magnitude of the local wind response is basically scaled by the magnitude of the local wind stress (τ_0) (e.g. Garvine, 1985; Wong, 1994; Janzen, 2000). The magnitude of the coastal sea level response to remote wind forcing on the continental shelf is also scaled by τ_0. Noble and Butman (1979) have estimated that an alongshelf wind stress of 0.1 Pa would produce a coastal sea level response of 0.17 m. Janzen (2000) used an estimate of 0.25 m coastal sea level per 0.1 Pa of wind stress in her modeling study to examine the effect of

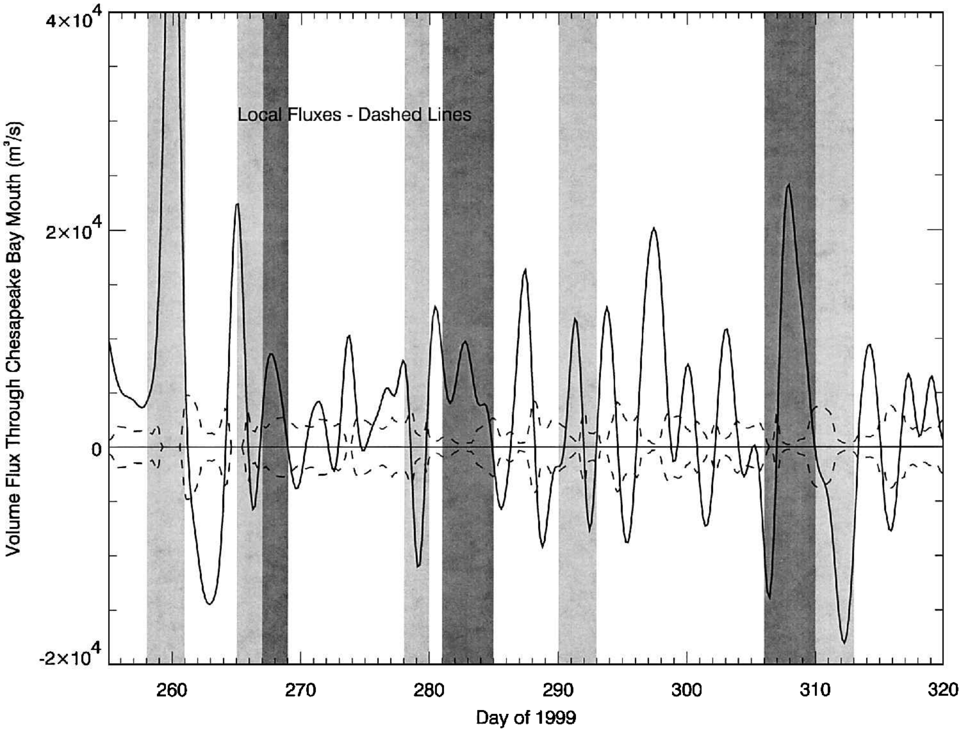

Figure 12. Same as in Figure 8 except for the autumn deployment.

remote wind forcing on the Delaware Bay. Given that the coastal sea level is scaled by τ_0, the current response at the entrance of an estuary to coastal sea level is scaled by $\omega\tau_0$, so the importance of the remote wind effect diminishes with decreasing frequency. It can be readily seen in the limiting, steady state case ($\omega \rightarrow 0$) that the remotely forced volume flux approaches zero while the locally forced response would still maintain downwind flow in part of the cross-section and upwind flow over the rest of the cross-section, as demonstrated by the analytical models of Officer (1976) and Wong (1994). This may in part contribute to the increased importance of the remote wind effect during the autumn deployment, as the characteristic frequency of the wind is higher in autumn than in spring. Secondly, the higher discharge in spring produces enhanced lateral and vertical salinity gradients relative to the conditions in autumn (Fig. 3). The increased vertical and lateral stratification may contribute to the enhancement of the bi-directional flow field associated with the local wind effect. This type of local wind-induced response has been observed in highly stratified systems such as the Mobile Bay (Noble *et al.,* 1996).

7. Summary

The major findings of this study of wind-induced exchange may be summarized as follows: (1) the temporal fluctuations in the barotropic volume flux associated with the coastally forced remote wind effect can be reasonably represented by the net flux integrated over the entire cross-section of the entrance to the estuary; (2) during the first deployment there is always a bi-directional exchange pattern (inflow and outflow existing simultaneously over different parts of the cross-section) superimposed on the sectionally averaged unidirectional exchange; (3) the magnitude of the bi-directional transport associated with the local wind effect may be a significant fraction of the unidirectional transport associated with the remote wind effect, and (4) the relative importance of the local wind effect in producing estuary-shelf exchange may change appreciably with season, depending on the characteristic frequency of the wind events and the degree of stratification in the estuary.

Acknowledgments. This work was funded by the U.S. National Science Foundation under grant OCE-9810649 to KCW and OCE-9812206 to AVL. We would like to express our deep appreciation to Kate Bosley for her contribution throughout the course of this study. Successful deployments and recoveries were accomplished with the help of many people and several vessels. The logistic support of R. Moody, R.C. Kidd, and A. Sundberg is greatly appreciated as well as the help of C. Reyes, A. Sepulveda, K. Holderied, R. Sanay, and M. Caceres. The NOAA/NOS field operations team provided invaluable support. Thanks to the crew of the NOAA ship, *Ferrel,* under the able command of LCDR Paul Moen, for their very professional support. Also, the crew of the *Sea Search* and the divers from Chesapeake Divers were crucial in the recovery efforts.

REFERENCES

Browne, D. R. and C. W. Fisher. 1988. Tide and tidal currents in the Chesapeake Bay, NOAA Tech. Rep. NOS OMA 3, U.S. Dept. of Commerce, Rockville, MD, 143 pp.

Chuang, W.-S. and W. C. Boicourt. 1989. Resonant seiche motion in the Chesapeake Bay. J. Geophys. Res., *94,* 2105–2110.

Csanady, G. T. 1973. Wind-induced barotropic motion in long lakes. J. Phys. Oceanogr., *3,* 429–438.

Doyle, B. E. and R. E. Wilson. 1978. Lateral dynamic balance in the Sandy Hook to Rockaway Point transect. Estuar. Coast. Mar. Sci., *6,* 165–174.

Elliott, A. J. 1978. Observation of the meteorologically induced circulation in the Potomac estuary. Estuar. Coast. Mar. Sci., *6,* 285–299.

Fischer, H. B. 1996. Mixing and dispersion in estuaries. Annu. Rev. Fluid Mech., *8,* 107–133.

Friedrichs, C. T. and J. M. Hamrick. 1996. Effects of channel geometry on cross sectional variations in along channel velocity in partially stratified estuaries, *in* Buoyancy Effects on Coastal and Estuarine Dynamics, Coastal and Estuarine Studies, *53,* American Geophysical Union, 283–300.

Garvine, R. W. 1985. A simple model of estuarine subtidal fluctuations forced by local and remote wind stress. J. Geophys. Res., *90,* 11,945–11,948.

—— 1991. Subtidal frequency estuary-shelf interaction: Observations near Delaware Bay. J. Geophys. Res., *96,* 7,049–7,064.

Geyer, W. R. 1997. Influence of wind dynamics and flushing of shallow estuaries. Estuar. Coast. Shelf Sci., *44,* 713–722.

Gill, A. E. and E. H. Schumann. 1974. The generation of long shelf waves by the wind. J. Phys. Oceanogr., *4,* 83–90.

Glorioso, P. D. and A. M. Davies. 1995. The influence of eddy viscosity formulation, bottom topography, and wind wave effects upon the circulation of a shallow bay. J. Phys. Oceanogr., *25,* 1243–1264.

Goodrich, D. M. 1987. Nontidal exchange processes at the Chesapeake Bay entrance. Proceedings of the 1987 National Conference on Hydraulic Engineering HY Div., ASCE, Williamsburg, VA, 493–498.

—— 1988. On meteorologically induced flushing in three U.S. east coast estuaries. Estuar. Coast. Shelf Sci., *26,* 11–121.

Goodrich, D. M., W. C. Boicourt, P. Hamilton and D. W. Pritchard. 1987. Wind-induced destratification in Chesapeake Bay. J. Phys. Oceanogr., *17,* 2232–2240.

Hearn, C. J., J. R. Hunter and M. L. Heron. 1987. The effects of a deep channel on the wind-induced flushing of a shallow bay or harbor. J. Geophys. Res., *92,* 3913–3924.

Hunter, J. R. and C. J. Hearn. 1987. Lateral and vertical variations in the wind-driven circulation in long, shallow lakes. J. Geophys. Res., *92,* 13,106–13,114.

Ianniello, J. P. 1977. Tidally induced residual currents in estuaries of constant breadth and depth. J. Mar. Res., *35,* 755–786.

—— 1979. Tidally induced residual currents in estuaries of variable breadth and depth. J. Phys. Oceanogr., *9,* 962–974.

Janzen, C. D. 2000. Wind forced dynamics of an estuary-shelf regime: Delaware Bay and the adjacent inner shelf. Ph.D. dissertation, University of Delaware, 216 pp.

Janzen, C. D. and K.-C. Wong. 2002. Wind forced dynamics at the estuary-shelf interface of a large coastal plain estuary. J. Geophys. Res., (in press).

Kalkwijk, J. P. T. and R. Booij. 1986. Adaptation of secondary flow in nearly-horizontal flow. J. Hydraul. Res., *24,* 19–37.

Kjerfve, B., J. E. Greer and R. L. Crout. 1978. Low-frequency response of estuarine sea level to non-local forcing, *in* Estuarine Interactions, M. L. Wiley, ed., Academic Press, 497–513.

Kjerfve, B. and B. A. Knoppers. 1991. Tidal choaking in a coastal lagoon, *in* Tidal Hydrodynamics, B. Parker, ed., John Wiley, 169–181.

MacCready, P. 1999. Estuarine adjustment to changes in river flow and tidal mixing. J. Phys. Oceanogr., *29,* 708–726.

Münchow, A., A. K. Masse and R. W. Garvine. 1992. Astronomical and nonlinear tidal currents in a coupled estuary shelf system. Cont. Shelf Res., *12,* 471–498.

Noble, M. and B. Butman. 1979. Low frequency wind-induced sea level oscillations along the east coast of North America. J. Geophys. Res., *84,* 3227–3236.

Noble, M. A., W. W. Schroeder, W. J. Wiseman Jr., H. F. Ryan and G. Gelfenbaum. 1996. Subtidal circulation patterns in a shallow, highly stratified estuary: Mobile Bay, Alabama. J. Geophys. Res., *101,* 25,689–25,703.

Officer, C. B. 1976. Physical Oceanography of Estuaries (and Associated Coastal Waters), John Wiley, NY, 465 pp.

Ou, H. W., R. C. Beardsley, D. Mayer, W. C. Boicourt and B. Butman. 1981. An analysis of the subtidal current fluctuations in the Middle Atlantic Bight. J. Phys. Oceanogr., *11,* 1383–1392.

Paraso, M. C. and A. Valle-Levinson. 1996. Meteorological influences on sea level and water temperature in the lower Chesapeake Bay: 1992. Estuaries, *19,* 548–561.

Pollak, M. J. 1960. Wind set-up and shear-stress coefficient in Chesapeake Bay. J. Geophys. Res., *65,* 3383–3389.

Reyes-Hernandez, A. C. 2001. Tidal and subtidal lateral structures of the density and velocity in the Chesapeake Bay entrance. Ph.D. dissertation, Old Dominion University, Norfolk, VA, 139 pp.

Schroeder, W. W. and W. J. Wiseman Jr. 1986. Low-frequency shelf-estuarine exchange process in Mobile Bay and other estuarine systems on the northern Gulf of Mexico, *in* Estuarine Variability, D. A. Wolfe, ed., Academic Press, 355–367.

Signell, R. P., R. C. Beardsley, H. C. Grabor and A. Capotondi. 1990. Effect of wave-current interaction on wind-driven circulation in narrow, shallow embayments. J. Geophys. Res., *95,* 9671–9678.

Smith, N. P. 1977. Meteorological and tidal exchange between Corpus Christi Bay, Texas and the northwestern Gulf of Mexico. Estuar. Coast. Mar. Sci., *5,* 511–520.

—— 1978. Long-period, estuarine-shelf exchange in response to meteorological forcing, *in* Hydrodynamics of Estuaries and Fjords, J. C. J. Nichoul, ed., Elsevier, 147–159.

Thorne, C. R. and R. D. Hey. 1979. Direct measurements of secondary currents at a river inflection point. Nature, *280,* 226–228.

Valle-Levinson, A. 1995. Observations of barotropic and baroclinic exchanges in the lower Chesapeake Bay. Cont. Shelf Res., *15,* 1631–1647.

Valle-Levinson, A. and K. M. M. Lwiza. 1998. Observations on the influence of downwelling winds on the Chesapeake Bay outflow, *in* Physics of Estuaries and Coastal Seas, J. Dronkers and M. Scheffers, eds., A. A. Balkema, Rotterdam, 247–256.

Valle-Levinson, A., C. Li, T. Royer and L. Atkinson. 1998. Flow patterns at the Chesapeake Bay entrance. Cont. Shelf Res., *18,* 1157–1177.

Valle-Levinson, A., K.-C. Wong and K. Bosley. 2000. Response of the lower Chesapeake Bay to forcing from Hurricane Floyd, Extended Abstracts from the 10th International Biennial Conference on Physics of Estuaries and Coastal Seas, C. Friedrichs and A. Valle-Levinson, eds., SRAMSOE Report No. 366, VIMS, Gloucester Point, VA, 119–122.

—— 2001. Observations of the wind-induced exchange at the entrance to Chesapeake Bay. J. Mar. Res., *59,* 391–416.

Vieira, M. E. C. 1985. Estimates of subtidal volume flux in mid Chesapeake Bay. Estuar. Coast. Shelf Sci., *21,* 411–427.

—— 1986. The meteorologically driven circulation in mid-Chesapeake Bay. J. Mar. Res., *44,* 473–493.

Walters, R. A. 1982. Low-frequency variations in sea level and currents in south San Francisco Bay. J. Phys. Oceanogr., *12,* 658–668.

Walters, R. A. and J. W. Gartner. 1985. Subtidal sea level and current variations in the northern reach of San Francisco Bay. Estuar. Coast. Shelf Sci., *21,* 17–32.

Wang, D.-P. 1979a. Subtidal sea level variations in Chesapeake Bay and relations to atmospheric forcing. J. Phys. Oceanogr., *9,* 413–421.

—— 1979b. Wind driven circulation in the Chesapeake Bay, winter 1975. J. Phys. Oceanogr., *9,* 564–572.

—— 1979c. Low frequency variability on the Middle Atlantic Bight. J. Mar. Res., *37,* 683–697.

Wang, D.-P. and A. J. Elliott. 1978. Non-tidal variability in the Chesapeake Bay and Potomac River: evidence for non-local forcing. J. Phys. Oceanogr., *8,* 225–232.

Weisberg, R. H. 1976. The nontidal flow in the Providence River of Narragansett Bay: a stochastic approach to estuarine circulation. J. Phys. Oceanogr., *6,* 721–734.

Weisberg, R. H. and W. Sturges. 1976. Velocity observations in the west passage of Narragansett Bay: a partially mixed estuary. J. Phys. Oceanogr., *6,* 345–354.

Wiseman, W. J., Jr., W. W. Schroeder and S. P. Dinnel. 1988. Shelf-estuarine water exchange between the Gulf of Mexico and Mobile Bay, Alabama. Am. Fish. Soc. Symp., *3,* 1–8.

Wong, K.-C. 1994. On the nature of transverse variability in a coastal plain estuary. J. Geophys. Res., *99,* 14,209–14,222.

—— 2002. On the wind-induced exchange between Indian River Bay, Delaware and the adjacent continental shelf. Cont. Shelf. Res. (in press).

Wong, K.-C. and R. W. Garvine. 1984. Observations of wind-induced, subtidal variability in the Delaware estuary. J. Geophys. Res., *89,* 10,589–10,597.

Wong, K.-C. and J. E. Moses-Hall. 1998. On the relative importance of the remote and local wind effects on the subtidal variability in a coastal plain estuary. J. Geophys. Res., *103,* 18,393–18,404.

Wong, K.-C. and R. E. Wilson. 1984. Observations of low-frequency variability in Great South Bay and relations to atmospheric forcing. J. Phys. Oceanogr., *14,* 1893–1900.

Received: *17 September, 2001;* revised: *26 March, 2002.*